Remote-Controlled Hydrogel Depots for Time-Scheduled Vaccination

*Raphael J. Gübeli, Désirée Hövermann, Hanna Seitz, Balder Rebmann, Ronald G. Schoenmakers, Martin Ehrbar, Ghislaine Charpin-El Hamri, Marie Daoud-El Baba, Martin Werner, Martin Müller, and Wilfried Weber**

Remote-controlled drug depots represent a highly valuable tool for the timely controlled administration of pharmaceuticals in a patient compliant manner. Here, the first pharmacologically controlled material that allows for the scheduled induction of a medical response in mice is described. To this aim, a novel, humanized biohybrid material that releases its cargo in response to a small-molecule stimulus licensed for human use is developed. The functionality of the material in mice is demonstrated by the remote-controlled delivery of a vaccine against the oncogenic human papillomavirus type 16. It is shown that the biohybrid depot-mediated immunoprotection is equivalent to the classical multi-injection-based vaccination. These results indicate that this material can be used as a universal remote-controlled vehicle for the patient-compliant delivery of vaccines and pharmaceuticals.

1. Introduction

Implantable drug depots represent a highly valuable approach for the timely and local administration of drugs in a patient-compliant manner.[1,2] Such drug depots are either made of electrical or mechanical devices[3,4] or of polymer systems[5] in which the drug is embedded and released thereof in a pre-scheduled or on-demand manner. While electro-mechanical devices allow timed or remote-controlled release kinetics, polymer-based drug depots are mainly restricted to diffusion or degradation-based release[6] preventing the adjustment of the drug release rate to changing needs of the patient. This latter drawback was addressed by the development of stimulus-sensing polymer-based hydrogels that dissolve or swell in response to an externally applied stimulus, a process that can be used to subsequently trigger the release of a previously embedded drug.[7,8] Such stimuli-sensing materials hold high promises as remote controlled drug depots, as hydrogels show an excellent tissue compatibility based on their high water content and viscoelastic properties emulating the natural extracellular matrix.[9] However, stimuli-sensing hydrogels developed to date have not reached clinical application due to trigger stimuli that are hardly compatible with human physiology or due to hydrogel building blocks likely to cause adverse reactions. For example, most stimuli-sensing hydrogels react to changes in temperature[10] or pH[11] beyond the physiological limits or are responsive to the administration of antigens,[12,13] ions[14] or metabolites[15] at concentrations hardly achievable in a therapeutic setting. One step in overcoming this stimulus incompatibility was the development of drug-sensing hydrogels that rely on clinically approved inducer molecules at pharmacologically relevant concentrations.[8,16–18] Such hydrogels enabled the small molecule-triggered release of a model protein in mice, however, the remaining hydrogel building blocks still showed limited biocompatibility.[16] In order to overcome these challenges, a stimulus-sensing hydrogel system would be required in which the hydrogel is exclusively synthesized from clinically licensed material and where the stimulus molecule is approved for human use, is orally available, does not show pharmacological site effects and is not accidentally present in the diet.

R. J. Gübeli
Faculty of Biology
SGBM Spemann Graduate School of Biology and Medicine
University of Freiburg
Albertstrasse 19A, 79104 Freiburg, Germany
D. Hövermann, B. Rebmann,
Dr. R. G. Schoenmakers, Prof. W. Weber
Faculty of Biology
BIOSS Centre for Biological Signalling Studies
University of Freiburg
Schänzlestrasse 18, 79104 Freiburg, Germany
E-mail: wilfried.weber@biologie.uni-freiburg.de

H. Seitz, Prof. M. Müller
German Cancer Research Center (DKFZ)
Im Neuenheimer Feld 242, 69120 Heidelberg, Germany
Dr. M. Ehrbar
Department of Obstetrics
University Hospital Zurich
Frauenklinikstrasse 10, 8091 Zurich, Switzerland
Dr. G. Charpin-El Hamri, Dr. M. Daoud-El Baba
Université de Lyon
43 Boulevard du 11 Novembre 1918, 69622 Villeurbanne, France
Prof. M. Werner
University Medical Center
Institute of Pathology
University of Freiburg
Breisacherstrasse 115A, 79106 Freiburg, Germany

DOI: 10.1002/adfm.201300875

Hydrogels with such advantageous properties could be loaded with a drug of interest and embedded into the body. At the optimum point in time, the oral administration of a stimulus molecule would induce the dissolution of the material and the subsequent release of the drug cargo. Such a scenario might be used to replace repetitive injections of a drug by one injection of the depot and the subsequent administration of an orally available tablet.[18,19] Prototype interventions requiring repeated injections are vaccines, where the first dose primes the immune system and the second and/or third dose boosts the immune response to protective titers. Despite the high preventive value of such vaccinations, a significant percentage of the population is not well protected as they missed the boost vaccination, either by the absence of qualified medical personnel or by negligence.[20] For example, 19% of US children were missing one or more doses of the recommended standard vaccinations.[21] In the case of the vaccine against human papilloma virus even more than 50% of the initiated vaccination regimes were not completed as prescribed likely resulting in reduced protection against this oncogenic infectious disease.[22] The success of such vaccination campaigns could likely be increased by the development of a new vaccination regime in which the first injection includes the prime vaccine and a hydrogel-based drug depot containing the boost dose. At the optimum point in time the simple administration of an orally available tablet would induce the release of the boost dose and trigger high immunoprotection.

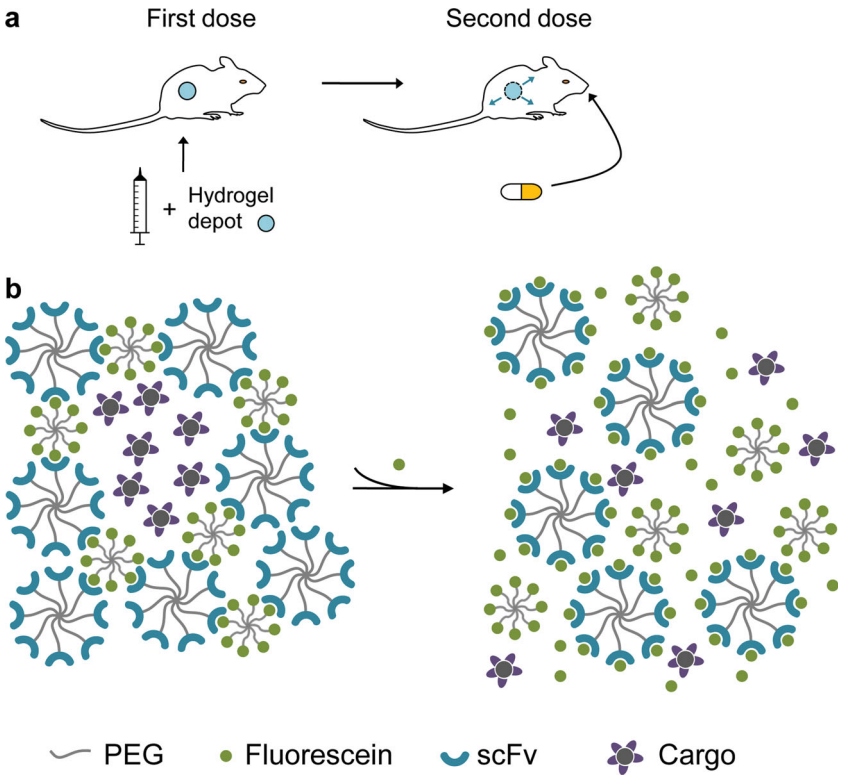

Figure 1. Design of the remote-controlled drug depot. a) The drug-loaded hydrogel depot is administered together with the first injection-based dose of the drug. For administering the second drug dose, an orally available small molecule is administered that triggers the dissolution of the hydrogel and the subsequent release of the drug cargo. b) Design of the small molecule-triggered hydrogel drug depot. The hydrogel is based on the specific interaction of a humanized single-chain variable fragment (scFv) with its binding partner, the human use-licensed contrast agent fluorescein. Hydrogel formation is induced by coupling the scFv and fluorescein to eight-arm polyethylene glycol (PEG). A cargo drug is physically entrapped into the hydrogel and inducibly released thereof by the addition of free fluorescein competing with the binding of fluorescein-PEG to the scFv.

In this study we developed such a one-injection-based vaccination regime against the high-risk oncogenic human papilloma virus type 16 (HPV16).[23] To this aim, we designed a novel hydrogel type exclusively based on parts commonly used in human therapy like polyethylene glycol, a humanized single-chain antibody fragment (scFv) as well as the clinically approved contrast agent fluorescein, which shows an excellent safety profile and has no targeted pharmacological effects.[24] We demonstrated that this hydrogel is suitable for the incorporation of the HPV16 vaccine, can be implanted into mice and triggered to release the cargo vaccine by the oral administration of fluorescein. We showed that this trigger-inducible approach gives rise to immunoprotection comparable to injection-based vaccination and therefore validates the utility of the novel hydrogel as remote-controlled drug depot for replacing repetitive injections by orally available medication.

2. Results and Discussion

We designed a hydrogel drug depot that dissolves upon administration of an orally available small molecule inducer for the remote-controlled administration of therapeutics (**Figure 1**a). To maximize biocompatibility and reduce the risk of adverse reactions, we restricted the choice of building blocks to molecules routinely used in the clinics like polyethylene glycol (PEG),[25] humanized single-chain antibody fragments[26] as well as the orally available, well-tolerated contrast agent fluorescein as human-use licensed inducer without pharmacological activity.[24] The hydrogel consisted of 8-arm PEG (M_W = 40 kDa) functionalized with a humanized fluorescein-specific single chain variable fragment[27] that was physically crosslinked to a hydrogel by 8-arm PEG-fluorescein (Figure 1b). The administration of free fluorescein competitively inhibited the interaction of both polymers and resulted in the dissolution of the hydrogel where such dissolution triggered the release of a previously entrapped cargo drug (Figure 1b).

8-arm PEG-fluorescein was synthesized by reacting 8-arm PEG amine (M_W = 20 kDa) with fluorescein isothiocyanate (FITC) resulting in the functionalization of 75% of the amine groups (Supporting Information Figure S1). The fluorescein-specific humanized scFv was recombinantly produced (Supporting Information Figure S2) with a C-terminal cysteine and mixed with 8-arm PEG-fluorescein at a 1:1 stoichiometry

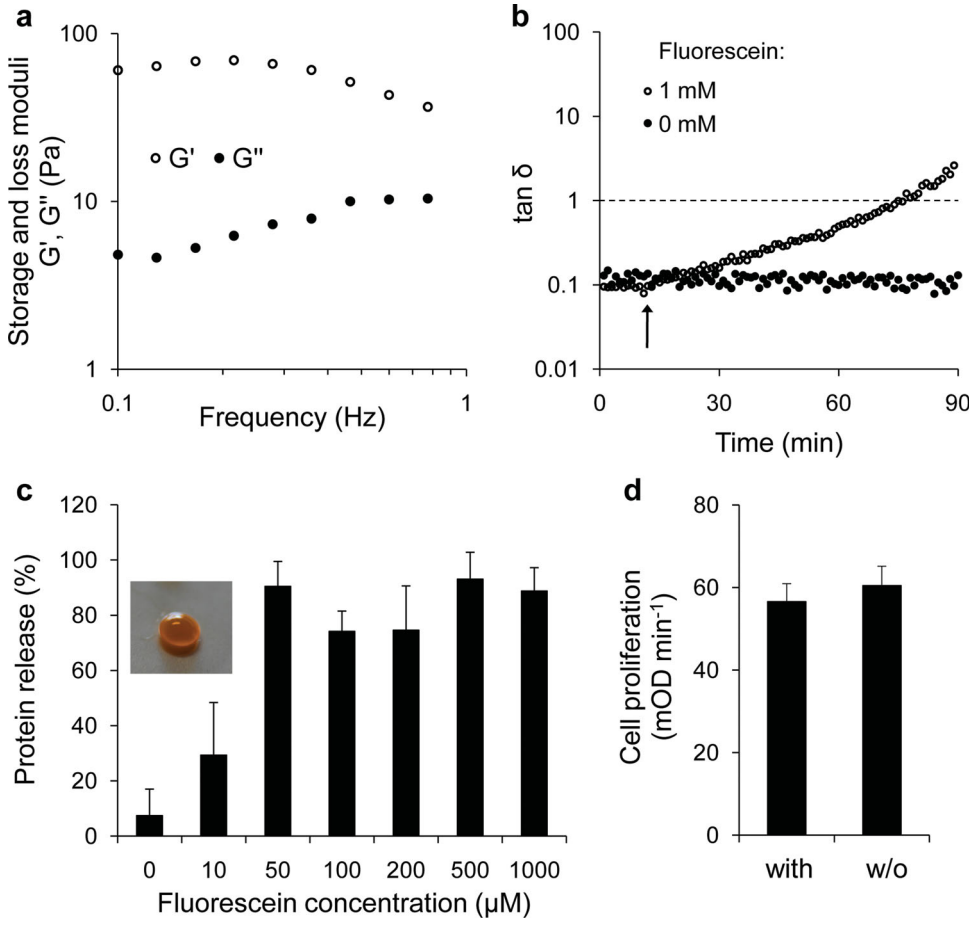

Figure 2. Characterization of the remote controlled hydrogel drug depot. a) Mechanical characterization of the hydrogel. Hydrogel discs (20 µL volume, 1 mm height) were prepared and pre-swollen in PBS for 1 h prior to determining the storage and loss moduli G′ and G″ by small-strain shear rheometry at frequencies from 0.1 to 1 Hz. b) Responsiveness of the hydrogel to fluorescein. Hydrogels (20 µL volume, 1 mm height) were prepared and pre-swollen for 1 h in PBS. The damping tan $\delta = G''/G'$ was determined at a constant frequency (0.5 Hz) by small-strain shear rheometry during 90 min. After 12 min (arrow), the buffer surrounding the hydrogel was exchanged to buffer optionally containing 1 mM fluorescein. c) Fluorescein-inducible dose-dependent hydrogel dissolution. Hydrogels (5 µL volume, picture inset) were preswollen in PBS and subsequently transferred to fresh PBS containing increasing concentrations of fluorescein. Hydrogel dissolution was monitored by quantifying the released scFv into the supernatant after 3 h. Error bars represent the standard deviation of 5 replicas. d) Cell culture compatibility of the hydrogel. 6000 human embryonic kidney (HEK-293T) cells were incubated in 200 µL medium in the presence (with) or absence (w/o) of a hydrogel (5 µL). Cell proliferation was assayed after 48 h by the WST-1 assay. Error bars represent the standard deviation of 6 replicas.

(scFv: fluorescein). Hydrogels were subsequently formed by the addition of vinylsulfone-functionalized 8-arm PEG (PEG-VS, M_W = 40 kDa) that specifically binds to thiol-containing cysteines in a Michael-type addition reaction.[28] In order to determine optimum synthesis parameters, increasing amounts of PEG-VS were added to PEG-fluorescein-scFv (vinylsulfone: scFv = 1:1–3:1; mol:mol) and the resulting hydrogels were preswollen in phosphate-buffered saline (PBS, pH 7.4) for 12 h. The hydrogels were subsequently transferred to fresh buffer and incubated for 24 h in the absence or presence (1 mM) of fluorescein prior to analyzing gel dissolution by quantifying the released scFv building blocks in the buffer supernatant (Supporting Information Figure S3). At a molar ratio of vinylsulfone: scFv = 2.5:1, complete dissolution was observed in the presence of fluorescein while leaky dissolution was in the order of 10%. These conditions corresponding to hydrogels (5 µL volume) containing 150 µg scFv (5.2 nmol), 19.4 µg PEG-fluorescein (5.2 nmol fluorescein groups) and 65 µg PEG-VS (13 nmol vinylsulfone groups) were chosen for the subsequent experiments in this study.

We characterized the mechanical and functional properties of the material as well as its cell culture compatibility. The viscoelastic properties of the material were determined by frequency-sweep experiments in the range of 0.1 to 1 Hz revealing a storage modulus G′ = 60.5 largely exceeding the loss modulus G″ = 4.8 at 0.1 Hz (**Figure 2**a). In order to evaluate the impact of fluorescein on the viscoelastic properties of the material, the damping (tan δ) was determined (Figure 2b, raw data in Supporting Information Figure S4) in time-sweep experiments. Directly after the addition of fluorescein (t = 12 min), a steady increase in tan δ was observed reaching the gel-to-sol transition after 65 min (tan δ = 1). This transition translates into

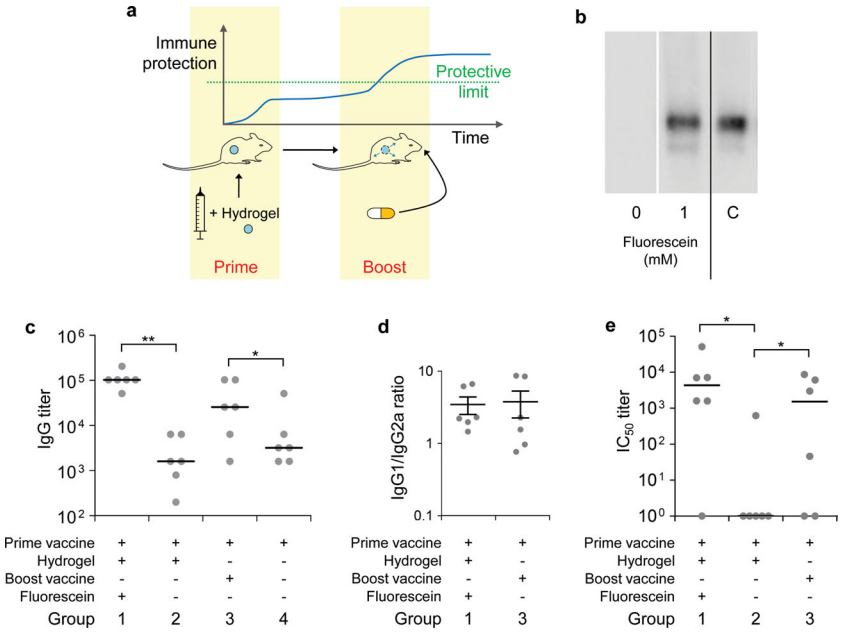

Figure 3. Remote-controlled hydrogel-mediated prime-boost vaccination against HPV16. a) Schematic representation of the vaccination regime. The prime vaccine dose is applied together with the vaccine-containing hydrogel depot. For boosting the immune response, the inducer molecule fluorescein is orally applied and triggers the release of the vaccine from the depot. b) Fluorescein-induced release of the vaccine from the hydrogel drug depot. Hydrogels (5 µL volume) were loaded with 0.5 µg alum-adsorbed HPV16 capsomeres and incubated in 1 mL PBS in the absence or presence of 1 mM fluorescein. After 3 h the released alum-adsorbed capsomeres were resolved by SDS-PAGE and analyzed by Western blotting using an anti-HPV16 L1 antibody. As control (C), 0.1 µg ml^{-1} alum-adsorbed capsomeres were loaded. c) Prime-boost vaccination in mice. All mice received a prime vaccine injection of 2 µg alum-adsorbed HPV16 capsomeres on day 1. Mice of groups 1 and 2 further subcutaneously received hydrogel depots (20 µL volume) harboring 2 µg alum-adsorbed HPV16 capsomeres. Mice of group 1 received oral fluorescein (20 mg per mouse) on day 6 (2 doses), 7 and 8 (1 dose each). Group 3 further received 2 µg alum-adsorbed HPV16 capsomeres by injection at day 7. At day 21, serum was withdrawn and reciprocal HPV-16-specific IgG titers were determined by ELISA. The median of the IgG titers is shown. * indicates differences in the median at a level of significance with $p < 0.05$; ** corresponds to $p < 0.01$. d) Sub-isotyping analysis of the HPV16-specific IgG response. The relative ratios of the IgG1 and IgG2a subtypes of the HPV16-specific IgGs were determined by ELISA. The horizontal bars represent the mean values, the error bars represent the standard error of the mean. e) Neutralization of HPV16 pseudovirions. Serum samples of day 63 were analyzed for their neutralization capacity of HPV16 pseudovirions. Serial dilutions of the serum were incubated with pseudovirions and subsequently applied to a HeLa-based reporter cell line expressing Gaussia luciferase upon pseudovirion infection. After 48 h the luciferase signal was used to determine the serum dilution at which 50% of the pseudovirions were inhibited (IC_{50}). IC_{50} titers are represented as the reciprocal serum dilution, median values are indicated by horizontal bars. * indicates differences in the median at a level of significance with $p < 0.05$.

the dissolution of the hydrogel as observed in a dose-response study revealing complete dissolution at 50 µM fluorescein after 3 h (Figure 2c).

Such a fluorescein profile needed for the complete dissolution of the hydrogel might also be achieved in vivo as the oral administration of fluorescein results in considerably high levels in the blood stream for 3–4 h[29] and diffuses well into the surrounding tissue.[24]

The hydrogel was further shown to be cell culture compatible as no significant difference in the proliferation of a model cell line (human embryonic kidney cells)[30] was observed over 48 h in the presence or absence of the material (5 µL gel per 200 µL culture volume, Figure 2d).

Based on the successful fluorescein-inducible dissolution of the hydrogel, we next analyzed whether this material could be applied as remote-controlled depot for the inducible administration of vaccines. Vaccines commonly require two or several injections over a period of several weeks in order to prime the immune system and to subsequently boost its response to immunoprotective levels (**Figure 3**a). In such a configuration a remote-controlled vaccine-releasing material would be of high value as it could replace the second injection and appointment at the physician by a simple orally available pill. We therefore characterized the suitability of our hydrogel as remote-controlled depot for a previously validated vaccine[31] against the oncogenic high-risk human papilloma virus type 16 (HPV16). For this we immobilized capsomeres derived from the viral L1 capsid protein on Alum that was subsequently added to the hydrogel synthesis mixture (0.1 µg capsomeres per µL gel volume) prior to the addition of crosslinking PEG-vinylsulfone. The vaccine-loaded hydrogels exhibited comparable mechanical properties to the original hydrogels (Supporting Information Figure S5) and did not show any detectable leaky release of the cargo upon incubation in PBS (Figure 3b). However, administration of fluorescein triggered the complete dissolution of the gels as determined by quantifying the hydrogel building blocks in the supernatant (Supporting Information Figure S6). This dissolution correlated with a quantitative release of the vaccine cargo as shown by Western blotting (Figure 3b). Furthermore, the electrophoretic behavior of the released vaccine was identical to control vaccine indicating that the capsomeres were not modified by the Michael-type addition reaction during hydrogel formation (Figure 3b).

Based on the successful trigger-inducible vaccine release studies we next validated the functionality of the hydrogel as remote-controlled drug depot in mice. In this configuration we aimed at replacing the second injection required for boosting the immune response by the oral intake of fluorescein to release the vaccine from the depot that has been administered together with the prime vaccination (Figure 3a). We therefore vaccinated the mice on day 1 with 2 µg alum-adsorbed HPV16 capsomeres and administered a vaccine-containing hydrogel (2 µg vaccine in a 20 µL gel) subcutaneously. The mice received fluorescein by oral route in 2 doses on day 6 and in 1 dose on day 7 and 8 to induce the dissolution of the gel depots and to release the vaccine (group 1, Figure 3c). In order to evaluate the effect of this remote-controlled release we used controls not receiving fluorescein (group 2, Figure 3c). For comparing this hydrogel-based vaccination strategy to

the conventional protocol, we used groups receiving classical prime-boost injections (day 1 and day 7) or a prime injection only (group 3 and 4, respectively, Figure 3c). The induction of the immune response was characterized on day 21 by determining HPV16 capsomere-specific IgG titers in the mouse serum (Figure 3c). The mice having received the prime vaccine, the vaccine depot and oral fluorescein (group 1) showed median IgG titers two orders of magnitude higher than mice lacking fluorescein administration (group 2) thereby confirming the functionality of the hydrogel depot and the remote-controlled release of bioactive vaccine. The median titers in the hydrogel-based prime-boost regime were comparable to the ones of the two-injection-based regime (group 3) thereby indicating that the bioactivity of the released vaccine has not been compromised. In mice having received the hydrogel depot but no fluorescein administration (group 2), the median IgG titers were comparable to the group having only received the prime vaccine (group 4) which indicates that the vaccine was not released from its depot in a non-specific manner. The same result was obtained by sampling mouse serum on day 63 (Supporting Information Figure S7) indicating the long-term effect of the immune-response.

The immune responses induced by depot-based or classical prime-boost regimes were further characterized by subtyping the HPV16-specific IgG antibodies being mainly responsible for Th2-lymphocyte mediated humoral immune responses (IgG1) and Th1-lymphocyte elicited cell-mediated responses (IgG2a) (Figure 3d and Supporting Information Figure S8). The ratios of the IgG1/IgG2a subtype levels showed a stronger Th2 response as typical for metal hydroxide mediated immunizations[32] and revealed no significant difference between the two delivery strategies indicating that the hydrogel immunization scheme did not alter the quality of the immune response.

We finally characterized the effectiveness of the induced immune reaction to protect against HPV16 infection in an in vitro pseudovirus neutralization assay (Figure 3e). To this aim, serial dilutions of the mouse sera (day 63) were incubated with HPV16 pseudovirions which were subsequently assayed for the infectivity in HeLaT reporter cells.[33] Both prime-boost strategies (groups 1 and 3), the hydrogel-based approach as well as the classical one showed comparable IC_{50} (half-maximum inhibitory concentration) median titers whereas mice lacking the fluorescein administration (group 2) did not show effective protection. These findings are in line with the IgG ELISA titers and indicate an equivalency with regard to therapeutic efficacy for the novel hydrogel-based and the classical injection-based regimes.

In order to analyze the tissue compatibility of the hydrogel depots, mice where sacrificed at day 8 and analyzed at the macroscopical and fine-histological level (**Figure 4**). Macroscopic analysis revealed an intact hydrogel in mice without fluorescein (group 2) while a strongly collapsed gel was observed in fluorescein-treated groups (group 1). Fine-histological analysis confirmed these observations revealing a compact gel in the control group and fragmented gel remnants in the fluorescein group. The histological analysis further revealed good tissue compatibility as no significant signs of inflammation or rejection were observed (Supporting Information Table S1).

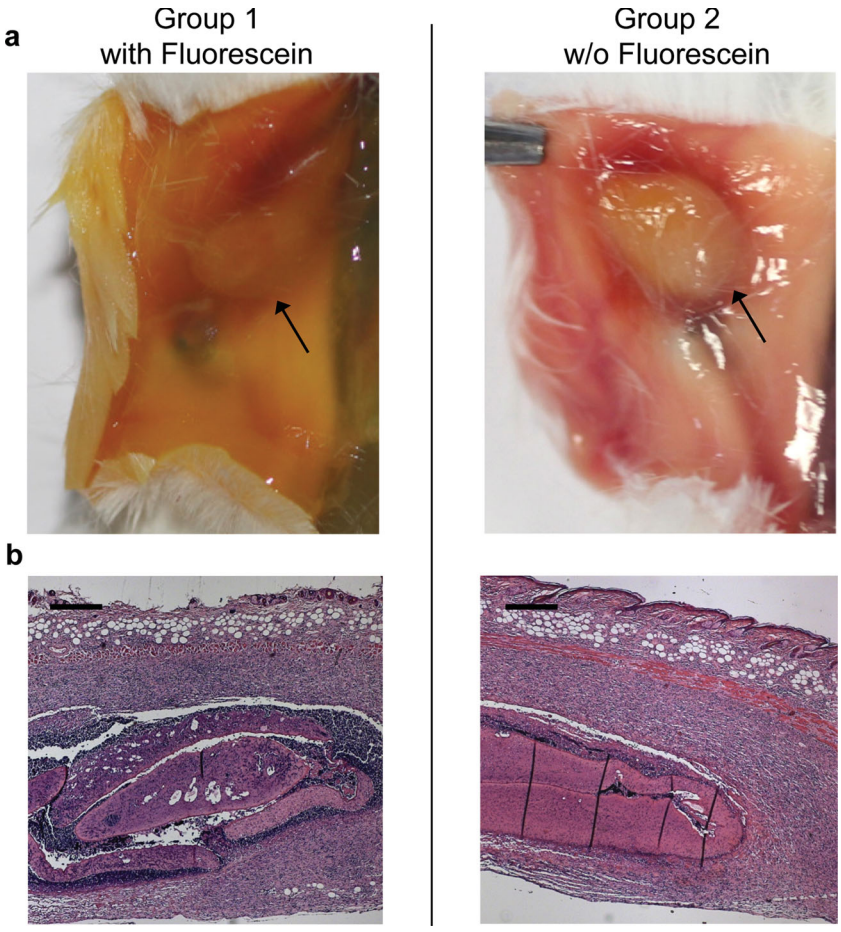

Figure 4. Macroscopic and histological characterization of the hydrogel depot. Mice of group 1 and 2 (see Figure 3c) were sacrificed at day 8 and the site of gel administration was analyzed. a) Macroscopic analysis of the gel implantation site. The hydrogel administration site is indicated by an arrow. b) Tissue sections through the centre of the hydrogel were stained with hematoxylin and eosin. Scale bars: 200 µm.

3. Conclusions

In this work we have developed a novel trigger-inducible hydrogel and demonstrated its functionality as remote-controlled vaccine depot in mice. With the synthesis of the hydrogel based on materials that are routinely used in the clinics, we overcame the major drawbacks of previous stimulus-sensing materials such as hardly compatible trigger stimuli or components likely to elicit adverse (immune) reactions. These characteristics together with the absence of contrast agents in a standard food regime makes

this class of molecules an ideal trigger stimulus for the remote-controlled activation of drug depots.

Beyond the specific implementation in this study, the design described here represents a rather generically applicable concept for the synthesis of stimulus-sensing materials. As scFvs can be obtained against virtually any small molecule using phage[34]- or ribosome[35] display, it is likely possible to adapt this concept to the development of materials with custom-tailored stimulus-responsiveness. Such a stimulus could be another externally administered molecule in the case of a remote controlled drug depot or it might as well be a physiological stimulus for the design of hydrogels that respond to (pathological) changes in the concentration of a metabolite or another disease-associated cue.

We have exemplified the in vivo functionality and compatibility of the hydrogel depot by the inducible release of an anti HPV16 L1-based vaccine thereby replacing a second vaccine injection by the oral intake of fluorescein. Given recent observations that up to 17% of the global population is not sufficiently protected with the few medically most important vaccines,[36] the remote-controlled vaccination strategy described in this study might be a suitable approach for increasing patient compliance and thus vaccination efficacy. This might especially be suitable for cases where general physicians are less available like in developing countries.

In order to allow for the simple intramuscular injection of the depot in humans similar to the commercially available HPV vaccines,[37] the presented vaccine depot may either be produced as an injectable microgel solution[38] or applied as instantly mixed precursor substances leading to gel depot formation in situ.[39]

As many vaccines are administered in alum-adsorbed form, the depot-based strategy described here will likely be generally applicable to other vaccines or even to other classes of pharmaceuticals like growth factors or antibodies that can easily be incorporated into biohybrid hydrogels.[40,41] Based on this flexibility in the cargo pharmaceutical combined with the potential of using different scFvs as described above, the present study likely represents a generic blueprint for the design of remote-controlled hydrogel drug depots for the patient compliant delivery of the ever growing number of biopharmaceuticals.

4. Experimental Section

Protein Production and Purification: The production and purification of cysteine-tagged scFv and the HPV16 capsomeres are described in the Supporting Information.

Synthesis of PEG-Fluorescein: 250 mg 8-arm PEG-NH_2 (20 kDa, Nanocs, New York, NY, cat. no. PG8A-AM-20k) was dissolved in 2.5 mL anhydrous dichloromethane and mixed with 97.35 mg (2.5 molar excess) fluorescein isothiocyanate (FITC, Sigma Aldrich, St. Louis, MO, cat. no. F7250) dissolved in 500 µL dichloromethane and 500 µL pyridine. The reaction was stirred at room temperature for 6 h followed by the addition of another 97.35 mg FITC (dissolved in 500 µL dichloromethane and 500 µL pyridine). After 18 h additional stirring, dichloromethane and pyridine were evaporated and the crude product was dissolved in 20 ml 100 mM ammonium carbonate pH 9. The PEG product was separated from low-molecular weight substances by ten dialysis cycles (12 h each) (SnakeSkin dialysis tubing, 3.5 kDa MWCO, Thermo Fisher Scientific) against 100 mM ammonium carbonate pH 9. The resulting product was lyophilized and stored at –80 °C. The fluorescein functionalization of the PEG amine end groups was 75% as determined by NMR (Supporting Information Figure S1). ^{1}H-NMR (CD3OD, 500 MHz) δ = 3.47–3.82 (m, CH_2CH_2O, PEG), 6.49 (dd, 2H fluorescein), 6.53 (m, 3H fluorescein), 7.13 (d, 1H fluorescein), 7.16 (d, 1H fluorescein), 7.19 (m, 1H fluorescein), 7.81 (m, 1H fluorescein) and 7.90 (m, 1H fluorescein).

Hydrogel Synthesis: The purified scFv(FITC-E2)-cys protein was concentrated to 20 mg mL^{-1} by ultrafiltration (10 kDa MWCO, Corning, Lowell, MA, cat. no. 431483), supplemented with a 20-fold molar excess of TCEP (Tris(2-carboxyethyl)phosphine hydrochloride, Sigma Aldrich, cat. no. C4706, 30 mg mL^{-1} in 500 mM sodium carbonate buffer pH 9) and incubated at room temperature for 1 h. Subsequently, the buffer was exchanged to hydrogel reaction buffer (2.68 mM KCl, 1.47 mM KH_2PO_4, 8.03 mM Na_2HPO_4, 137 mM NaCl, 2 mM ethylenediaminetetraacetic acid, pH 8) via a desalting column (Thermo Fisher Scientific, cat. no. 43233) and the protein was concentrated to 50 mg mL^{-1} by ultrafiltration (10 kDa MWCO, Corning, cat. no. 431483) under nitrogen atmosphere.

Typical hydrogels of 5 µL volume were produced by mixing 150 µg scFv(FITC-E2)-cys (5.2 nmol) with 19.4 µg PEG-fluorescein (equivalent to 5.2 nmol fluorescein) in 3.55 µL hydrogel reaction buffer and incubation for 1 h at room temperature. Subsequently, 65 µg 40 kDa 8-arm PEG-vinyl sulfone (equivalent to 13 nmol vinyl sulfone groups, 1.3 µL of 50 mg mL^{-1} in reaction buffer, obtained as described elsewhere)[42] and 0.15 µL 3.3 M triethanolamine pH 8 were added. The solution was subsequently spotted on siliconized (Sigmacote, Sigma Aldrich, cat. no. SL-2) glass slides and incubated at 25 °C for 24 h under a humidified atmosphere for gelation. The resulting hydrogels were incubated in PBS (2.68 mM KCl, 1.47 mM KH_2PO_4, 8.03 mM Na_2HPO_4, 137 mM NaCl, pH 7.4) supplemented with 100 mM ethanolamine for 1 h followed by incubation in PBS for 12 h.

For the synthesis of hydrogels harboring the HPV vaccine, 0.1 µg alum-adsorbed HPV 16 L1 capsomeres were added per µL final hydrogel volume to the hydrogel mix prior to the addition of PEG-vinyl sulfone.

Mechanical Hydrogel Characterization: For mechanical characterization, hydrogel discs of 20 µL volume were prepared between two siliconized glass slides (height 1 mm) and pre-swollen in PBS for 1 h. Small strain oscillatory shear experiments to obtain storage and loss moduli (G′ and G″) were performed on a modular advanced rheometry system II (Thermo Fisher Scientific) with 20 mm parallel steel plates at 20 °C. Swollen hydrogels were placed between the steel plates followed by adjustment of the gap to 0.5 mm and surrounding the hydrogel with PBS to prevent drying out. Frequency-sweep experiments were performed at a constant strain (20%) from 0.1 to 1 Hz. Time-sweep experiments were conducted at constant frequency (0.5 Hz) and constant strain (20%) by measuring storage and loss moduli as a function of time. The fluorescein responsiveness was analyzed by replacing the buffer with PBS optionally supplemented with 1 mM fluorescein after 12 min. The measurement was continued for 78 min.

Fluorescein-Induced Hydrogel Dissolution: Pre-swollen hydrogels (volume: 5 µL) were transferred to 1 mL PBS containing the indicated fluorescein concentrations. The stimulus-responsive dissolution was monitored by quantifying the released protein in the supernatant after 3 h using the Bradford method. Released HPV vaccine was specifically detected by resolving the buffer supernatant by 10% (wt/vol) SDS-PAGE and subsequent Western blotting using a mouse anti-HPV16 L1 antibody (Santa Cruz Biotechnology, Santa Cruz, CA, cat. no. sc-65713) and a secondary anti-mouse peroxidase antibody (GE Healthcare, Piscataway, NJ, cat. no. NA931V). Detection was performed using ECL-plus reagent (GE Healthcare, cat. no. RPN2132) on a LAS 4000 imager (Fujifilm Europe, Düsseldorf, Germany). 0.1 µg mL^{-1} alum-adsorbed capsomeres were used as control.

Cell Culture Compatibility Assay: For analyzing cell culture compatibility, hydrogels (5 µL volume) were prepared and pre-swollen in PBS for 12 h and subsequently added to 6 ' 000 HEK-293T cells cultivated in 200 µL Dulbecco's modified Eagle's medium (DMEM) supplemented with 10% vol/vol fetal calf serum (FCS, PAN Biotech, Aidenbach, Germany, cat. no. 3302-P281803) in a 96-well plate. After

48 h, mammalian cell proliferation was quantified by the tetrazolium salt-based WST-1 assay (Roche Applied Science, Rotkreuz, Switzerland, cat. no. 05015944001). For this aim, the hydrogels were removed and the reagent solution (10 vol%) was added to each cell-culture well. The kinetics of formazan formation were followed at 440 nm and 37 °C over 1 h in a plate reader.

Mice Vaccination Studies: For vaccination studies, female Swiss CD 1 mice (Janvier SAS CS 4105, Le Genest St Isle F-53941 St Berthevin, France) were used. Alum-adsorbed HPV capsomeres (2 µg) were resuspended in 100 µL PBS and subsequently injected. The vaccine-loaded hydrogel depot (2 µg alum-adsorbed HPV capsomeres per 20 µL hydrogel) was applied subcutaneously on the back of the mice under sodium pentobarbital (Nembutal) 6% anesthesia, 45 mg kg^{-1}. Fluorescein was dissolved at 125 mg mL^{-1} in 150 mM NaCl and applied at a dose of 20 mg per mouse at day 6 (2 doses), 7 and 8 (one dose each) by gastric tube. Serum samples were withdrawn on day 21 and 63. All animal experiments were performed according to the directives of the European Community Council (86/609/EEC), approved by the French Republic (no. 69266310).

Determination of the Serum IgG Titers: Serum IgG titers were determined using an HPV16 VLP capture ELISA as described previously.[31] In brief, 96-well ELISA plates (Corning, cat. no. 3590) were coated for 12 h with polyclonal rabbit IgG specific for HPV16 VLPs (85 ng/well). All following incubation steps were performed for 1 h at 37 °C. The wells were blocked using 300 µl/well blocking buffer (3% (wt/vol) skim milk powder in PBS), washed three times (PBS supplemented with 0.3% (wt/vol) Tween20) and supplemented with 350 ng HPV16 VLPs per well in blocking buffer. After three washing cycles, mouse sera were applied in a 2 x serial dilution in blocking buffer starting with a 1:200 dilution. After three washing cycles, a goat anti-mouse IgG horseradish peroxidase conjugate (Dianova, Hamburg, Germany, cat. no. 115-035-003, dilution 1:3000) was added in blocking buffer followed by three washing cycles and the addition of the colorimetric substrate (0.3 mg mL^{-1} ABTS (2,2′-azino-bis(3-ethylbenzthiazoline-6-sulfonic acid) and 0.006 vol% H_2O_2 in 100 mM sodium acetate pH 4) and quantification of absorbance at 405 nm in a plate reader. IgG titers were calculated as the reciprocal of the highest dilution giving an absorbance value above the cutoff value (the average for the negative control mice plus three times the standard deviation). IgG subisotype levels were determined using an ELISA with isotype-specific antibodies (Mouse Typer Isotyping Kit, Bio-Rad, cat. no. 172–2051) and initial coating with 350 ng/well of HPV16 VLPs. Mouse sera were diluted 1:400.

Neutralization Assay: Neutralization assays were performed as recently described.[33] Briefly, 50 µL of diluted serum samples were mixed with 50 µL of diluted pseudovirion stocks (end concentration of 2.4×10^5 viral genomes/well) and incubated at room temperature for 30 min. Next, 50 µL HeLaT cells[33] (2.5×10^5 cells mL^{-1}) were added to the pseudovirion-antibody mixture and incubated for 48 h at 37 °C and 5 vol% CO_2. The amount of secreted gaussia luciferase in 10 µL of cell culture medium was determined using coelenterazine substrate/gaussia glow juice (PJK, Kleinblittersdorf, Germany, cat. no. 102544) according to the manufacturer's instructions. A microplate luminometer (Victor^3, Perkin Elmer, Waltham, MA) was used to measure luminescence 15 min after substrate addition.

Histological Analysis: Mice of groups 1 and 2 were sacrificed on day 8. The skin of the subcutaneous implantation site was explanted, fixed in 4% (wt/vol) formalin for 24 h and embedded in paraffin. Serial 5 µm paraffin sections were stained for hematoxylin and eosin (HE), perjodic acid-Schiff stain (PAS), Elastica-van Gieson (EvG) and Prussian blue. The stained sections were analyzed using a bright field microscope (Axioplan, Zeiss, Oberkochen, Germany) equipped with 1, 25×, 5×, 10×, 20×, 40× and 63× objectives. Different types of inflammatory cells as well as granulomatous tissue surrounding the hydrogel implants were semiquantitatively assessed. Digital images were taken using a digital microscope camera.

Statistical Analysis: Statistical comparison among groups was performed by Mann-Whitney U test using Graphpad Prism 6 (Graphpad, La Jolla, CA). P values ≤ 0.05 were considered statistically significant.

Supporting Information

Supporting Information is available from the Wiley Online Library or from the author.

Acknowledgements

We thank Clément Moucheroud for assistance with the animal experiments. We would like to thank Carina Gillig and Christian Friedrich for support with the rheological characterization, Christian Hoischen for providing the plasmid pEA12 and the bacterial strain *P. mirabilis* LVI, Esther Kleiner for help with histology and Andreas Plückthun for providing the plasmid pAK400-FITC-E2. This work was supported by the European Research Council under the European Community's Seventh Framework Programme (FP7/2007-2013)/ ERC Grant agreement no. 324622-SmartVaccines and the Excellence Initiative of the German Federal and State Governments (EXC-294 and GSC-4).

Received: March 11, 2013
Revised: April 17, 2013
Published online: June 5, 2013

[1] D. A. LaVan, T. McGuire, R. Langer, *Nat. Biotechnol.* **2003**, *21*, 1184.
[2] B. P. Timko, T. Dvir, D. S. Kohane, *Adv. Mater.* **2010**, *22*, 4925.
[3] H. Buchwald, J. Barbosa, R. L. Varco, T. D. Rohde, W. M. Rupp, R. A. Schwartz, F. J. Goldenberg, P. J. Blackshear, *Lancet* **1981**, *2*, 360.
[4] D. Gershon, *Nat. Med.* **2012**, *18*, 506.
[5] M. A. C. Stuart, W. T. S. Huck, J. Genzer, M. Muller, C. Ober, M. Stamm, G. B. Sukhorukov, I. Szleifer, V. V. Tsukruk, M. Urban, F. Winnik, S. Zauscher, I. Luzinov, S. Minko, *Nat. Mater.* **2010**, *9*, 101.
[6] A. S. Hoffman, *Adv. Drug Delivery Rev.* **2002**, *54*, 3.
[7] J. S. Mohammed, W. L. Murphy, *Adv. Mater.* **2009**, *21*, 2361.
[8] J. Kopecek, J. Y. Yang, *Angew. Chem. Int. Ed.* **2012**, *51*, 7396.
[9] D. Seliktar, *Science* **2012**, *336*, 1124.
[10] B. Jeong, Y. H. Bae, D. S. Lee, S. W. Kim, *Nature* **1997**, *388*, 860.
[11] M. Torres-Lugo, N. A. Peppas, *Macromolecules* **1999**, *32*, 6646.
[12] T. Miyata, N. Asami, T. Uragami, *Nature* **1999**, *399*, 766.
[13] Z. R. Lu, P. Kopeckova, J. Kopecek, *Macromol. Biosci.* **2003**, *3*, 296.
[14] J. D. Ehrick, S. K. Deo, T. W. Browning, L. G. Bachas, M. J. Madou, S. Daunert, *Nat. Mater.* **2005**, *4*, 298.
[15] M. Watanabe, T. Akahoshi, Y. Tabata, D. Nakayama, *J. Am. Chem. Soc.* **1998**, *120*, 5577.
[16] M. M. Kampf, E. H. Christen, M. Ehrbar, M. Daoud-El Baba, G. Charpin-El Hamri, M. Fussenegger, W. Weber, *Adv. Funct. Mater.* **2010**, *20*, 2534.
[17] M. Ehrbar, R. Schoenmakers, E. H. Christen, M. Fussenegger, W. Weber, *Nat. Mater.* **2008**, *7*, 800.
[18] K. Jakobus, S. Wend, W. Weber, *Chem. Soc. Rev.* **2012**, *41*, 1000.
[19] W. Weber, M. Fussenegger, *Nat. Rev. Genet.* **2012**, *13*, 21.
[20] S. Anand, T. Barnighausen, *Lancet* **2007**, *369*, 1277.
[21] E. T. Luman, K. M. Shaw, S. K. Stokley, *Am. J. Prev. Med.* **2008**, *35*, 319.
[22] L. E. Widdice, D. I. Bernstein, A. C. Leonard, K. A. Marsolo, J. A. Kahn, *Pediatrics* **2011**, *127*, 77.
[23] D. R. Lowy, J. Kim, K. K. Smith-McCune, C. J. M. Melief, *Nat. Med.* **2012**, *18*, 28.
[24] K. O'Goshi, J. Serup, *Skin Res.* **2006**, *12*, 155.
[25] F. M. Veronese, G. Pasut, *Drug Discovery Today* **2005**, *10*, 1451.
[26] P. J. Carter, *Nat. Rev. Immunol.* **2006**, *6*, 343.
[27] T. J. Vaughan, A. J. Williams, K. Pritchard, J. K. Osbourn, A. R. Pope, J. C. Earnshaw, J. McCafferty, R. A. Hodits, J. Wilton, K. S. Johnson, *Nat. Biotechnol.* **1996**, *14*, 309.

[28] M. Morpurgo, F. M. Veronese, D. Kachensky, J. M. Harris, *Bioconjugate Chem.* **1996**, *7*, 363.
[29] A. G. Palestine, R. F. Brubaker, *Invest. Ophthamol. Visual Sci.* **1981**, *21*, 542.
[30] S. J. Shukla, R. L. Huang, C. P. Austin, M. H. Xia, *Drug Discovery Today* **2010**, *15*, 997.
[31] N. Thones, A. Herreiner, L. Schadlich, K. Piuko, M. Muller, *J. Virology* **2008**, *82*, 5472.
[32] J. C. Cox, A. R. Coulter, *Vaccine* **1997**, *15*, 248.
[33] H. Seitz, M. Schmitt, G. Bohmer, A. Kopp-Schneider, M. Muller, *Int. J. Cancer* **2013**, *132*, E139.
[34] T. Clackson, H. R. Hoogenboom, A. D. Griffiths, G. Winter, *Nature* **1991**, *352*, 624.
[35] J. Hanes, A. Pluckthun, *Proc. Natl. Acad. Sci. USA* **1997**, *94*, 4937.
[36] Centers for Disease Control and Prevention, *Morbidity and Mortality Weekly Report* **2012**, *61*, 883.
[37] L. A. Koutsky, D. M. Harper, *Vaccine* **2006**, *24*, 114.
[38] T. Rossow, J. A. Heyman, A. J. Ehrlicher, A. Langhoff, D. A. Weitz, R. Haag, S. Seiffert, *J. Am. Chem. Soc.* **2012**, *134*, 4983.
[39] S. Wechsler, D. Fehr, A. Molenberg, G. Raeber, J. C. Schense, F. E. Weber, *J. Biomed. Mater. Res. A* **2008**, *85A*, 285.
[40] P. S. Lienemann, M. Karlsson, A. Sala, H. M. Wischhusen, F. E. Weber, R. Zimmermann, W. Weber, M. P. Lutolf, M. Ehrbar, *Adv. Healthcare Mater.* **2013**, *2*, 292.
[41] B. Fejerskov, A. N. Zelikin, *Plos One* **2012**, 7.
[42] R. J. Gubeli, M. Ehrbar, M. Fussenegger, C. Friedrich, W. Weber, *Macromol. Rapid Commun.* **2012**, *33*, 1280.